

An opto-mechanical coupled-ring reflector driven by optical force for lasing wavelength control

Ren, M.; Cai, He; Chin, Lip Ket; Huang, Jianguo; Gu, Y. D.; Radhakrishnan, K.; Ser, Wee; Liu, Ai
Qun

2016

Ren, M., Cai, H., Chin, L. K., Huang, J., Gu, Y. D., Radhakrishnan, K., et al. (2016). An
opto-mechanical coupled-ring reflector driven by optical force for lasing wavelength
control. *Applied Physics Letters*, 108(8), 081106-.

<https://hdl.handle.net/10356/80745>

<https://doi.org/10.1063/1.4942505>

© 2016 American Institute of Physics (AIP). This paper was published in *Applied Physics Letters* and is made available as an electronic reprint (preprint) with permission of American Institute of Physics (AIP). The published version is available at: [<http://dx.doi.org/10.1063/1.4942505>]. One print or electronic copy may be made for personal use only. Systematic or multiple reproduction, distribution to multiple locations via electronic or other means, duplication of any material in this paper for a fee or for commercial purposes, or modification of the content of the paper is prohibited and is subject to penalties under law.

Downloaded on 25 Aug 2022 00:31:30 SGT

An opto-mechanical coupled-ring reflector driven by optical force for lasing wavelength control

M. Ren,^{1,2,a)} H. Cai,^{2,b)} L. K. Chin,¹ J. G. Huang,¹ Y. D. Gu,² K. Radhakrishnan,¹ W. Ser,¹ and A. Q. Liu^{1,b)}

¹*School of Electrical and Electronic Engineering, Nanyang Technological University, 50 Nanyang Avenue, Singapore 639798*

²*Institute of Microelectronics, A*STAR, 11 Science Park Road, Singapore 117685*

(Received 26 November 2015; accepted 9 February 2016; published online 23 February 2016)

In this paper, an opto-mechanical coupled-ring reflector driven by optical gradient force is applied in an external-cavity tunable laser. A pair of mutually coupled ring resonators with a free-standing arc serves as a movable reflector. It obtains a 13.3-nm wavelength tuning range based on an opto-mechanical lasing-wavelength tuning coefficient of 127 GHz/nm. The potential applications include optical network, on-chip optical trapping, sensing, and biology detection. © 2016 AIP Publishing LLC. [<http://dx.doi.org/10.1063/1.4942505>]

With the rapid development of the micro/nano wafer-fabrication technology, miniaturization of external cavity tunable lasers has been successfully developed and widely applied for optical communication, data processing, and sensing.¹ The tunability of the demonstrated lasers is mainly determined by the tuning components, such as gratings,^{2,3} ring resonators,^{4,5} and movable mirrors.^{6–9} For wavelength tuning, electrical circuits are utilized to control the tunable components and provide feedback to the laser system through multiple electrically tuning schemes. For example, thermal-optic³ or free-carrier dispersion^{4,5} effects have been adopted to tune the effective refractive index in waveguide-based tunable lasers, or electrostatic effect has been applied to tune the cavity length or the position of the movable mirrors in the micro-electromechanical systems (MEMS) tunable lasers.^{6–9} All these require complex electrical circuits to provide a signal feedback to the laser system and consume additional electrical power on these tuning components. Therefore, an all-optical solution of wavelength tuning is desired, as a significant innovation, for the external cavity tunable lasers. The optically tuning manner, which is compatible to on-chip integration, is made possible by applying the opto-mechanical effect. Nanoscale positioning is achievable, since optical gradient force is exerted on the free-standing waveguide when light is evanescently coupled to a nearby waveguide or a dielectric substrate,^{10,11} and the effective refractive index of the free-standing waveguide is changed with the nanoscale position.^{12–16} The amplitude of the optical gradient force depends on the gradient of the electromagnetic field and is significantly enhanced by the ring resonators with high quality factor.^{14–16}

In this paper, an opto-mechanical coupled-ring reflector driven by optical force is proposed for lasing wavelength tuning in an external-cavity tunable laser. A pair of coupled ring resonators with a free-standing arc serves as an opto-mechanical movable mirror. The lasing wavelength is controlled by optical force. Since the optical force is originated from the lasing light in the laser cavity, this optically controlled scheme gets rid of the dependence on electric power consumption on the tuning components, paving ways for all-optical photonic system.

Figure 1 shows the opto-mechanical coupled-ring reflector in the external cavity tunable laser. It consists of a gain chip and an opto-mechanical reflector, which are connected by a nano-silicon bus waveguide. The reflector consists of two mutually coupled ring resonators, being coupled to the bus waveguide. Ring 1 serves as a driving ring, which is partially released to form a free-standing arc and its resonant wavelength is tuned by arc deformation controlled by optical gradient force. Ring 2 with constant effective refractive index serves as the reference ring. The specific wavelength, which meets the resonances of both rings to obtain the highest reflectivity, determines the resonant wavelength. When one of the longitudinal modes of the entire laser cavity matches with the central resonance of the opto-mechanical coupled-ring reflector, it is selected as the lasing wavelength. Since the lasing light oscillates in the laser cavity and is coupled to the ring resonators through the bus waveguide, the free-standing arc is deflected with a deformation x by the optical gradient force. Consequently, the effective refractive index of ring 1 and the central resonance of the opto-mechanical coupled-ring reflector are changed, which provide an optical feedback to the laser system for lasing wavelength control. At a certain intra-cavity optical power, the stable lasing wavelength is obtained when the force balance

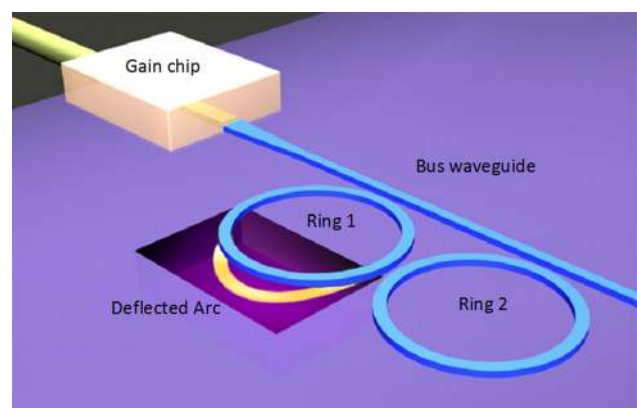


FIG. 1. Schematic illustration of the opto-mechanical coupled-ring reflector driven by optical gradient force in an external-cavity tunable laser, where the lasing wavelength is optically tuned through deflecting the free-standing arc of the driving ring.

^{a)}Present address: Data Storage Institute, A*STAR, Singapore.

^{b)}caih@ime.a-star.edu.sg and eaqliu@ntu.edu.sg.

between the optical gradient force and the mechanical force (due to the arc stiffness) is satisfied. The amount of wavelength tuning is dependent on the change of the intra-cavity optical power. The radii of ring 1 and ring 2 are 30 and 29 μm , respectively. The nano-silicon waveguides have a dimension of 450 nm in width and 220 nm in height. The coupling gap between the ring and the bus waveguide is 200 nm, and the gap between the pair of the coupling ring is 330 nm. The reflective properties of the coupled-ring reflector are calculated by using the Transfer Matrix Method,¹⁷ whereby the power coupling coefficient of the ring-bus and ring-ring coupling are chosen as 0.16 and 5×10^{-4} , respectively, considering the requirement for both high reflectivity and high wavelength selectivity. The effective refractive index of the silicon waveguide (TE mode) with silicon dioxide (SiO_2) cladding is set to 2.79, and the optical loss of the silicon waveguide is set to 1.5 dB/cm. The calculated reflectivity of the coupled-ring reflector $r_c(\lambda)$ is $\sim 80\%$, and the margin between the main resonance and the side resonance is ~ 2.6 dB. The taper waveguide is used to obtain the mode-size matching between the gain chip (with its right facet anti-reflective coated) and the bus waveguide.

In ring 1, the air gap between the free-standing arc and the SiO_2 layer is $g_0 = 160$ nm. The lasing light in the laser cavity generates an optical gradient force to deflect the arc. When the free-standing arc is bent towards the SiO_2 layer with a central deflection x , the air gap is changed to $g = g_0 - x$. The effective refractive index of the arc n_{eff} increases when the air gap is reduced. Consequently, the resonant wavelength of ring 1, λ_r , is red-shifted. The opto-mechanical resonance tuning coefficient of ring 1 is exponentially fit to $\frac{\partial \lambda_r}{\partial x} = A_1 \exp(A_2 x)$, where $A_1 = 2.3 \times 10^{-2}$ and $A_2 = 1.35 \times 10^{-2}$ at an initial gap of 160 nm. The optical force which acts on the free-stand arc is expressed as¹⁶

$$F_{\text{opt}} = - \frac{2\tau_e^{-1} P_b}{(\lambda_L - \lambda_r)^2 (2\pi c)^2 \lambda_r^{-3} + \lambda_r (\tau_i^{-1} + \tau_e^{-1})^2} \frac{\partial \lambda_r}{\partial x}, \quad (1)$$

where P_b is the intra-cavity optical power, $1/\tau_e = 2.1 \times 10^{10}$ Hz is the extrinsic decay rate of ring 1 due to the externally coupling, $1/\tau_i = 1.1 \times 10^{10}$ Hz is the intrinsic decay rate due to the internal ring resonator loss, and λ_L is the lasing wavelength. Difference from previously demonstrated single opto-mechanical ring whereby the deformation of the free-standing arc is controlled by adjusting the wavelength of the external light,¹⁶ the opto-mechanical coupled-ring reflector serves as a self-adaptive mirror using two mutually coupled ring resonators in which the deformation of the free-standing arc is controlled by the intra-cavity optical power of the laser. The deflection x adjusts the central reflective wavelength of the opto-mechanical coupled-ring reflector due to the change of refractive index and provides a feedback to the lasing wavelength of the tunable laser λ_L . Therefore, the detuning between the resonance λ_r of ring 1 and the lasing wavelength λ_L is nearly zero. In addition, the achievable resonance tuning of the coupled-ring reflector is amplified due to the Vernier effect, as compared with the resonance tuning of a single opto-mechanical ring, from a few to tens of nanometers. The deflected deformation x of the free-standing arc

corresponding to different intra-cavity powers is analyzed as shown in Fig. 2(a). The mechanical force ($F_{\text{mech}} = kx$) increases linearly with x , where $k = 0.14$ N/m is the mechanical spring constant of the free-standing arc, while the optical force $|F_{\text{opt}}(x)|$ increases nonlinearly with x . In general, F_{mech} and $|F_{\text{opt}}|$ intersect once or twice, and the static force equilibrium is obtained when the optical force balances the mechanical force at points $a-d$ as shown in Fig. 2(a). According to stability analysis, points $a-c$ are stable deflection positions, while point d is unstable. Thus, the opto-mechanical tuning is controllable when the intra-cavity power is below 5.6 mW.

The tuning of the lasing wavelength is amplified by a factor $M = \frac{R_1}{\Delta R}$ as compared with the resonance tuning of ring 1, where $R_1 = 30 \mu\text{m}$ is the radius of ring 1 and $\Delta R = 1 \mu\text{m}$ is the radii difference between the two ring resonators. The achievable tuning range $\Delta\lambda_{\text{tune}}$ of the tunable laser is expressed as

$$\Delta\lambda_{\text{tune}} = \frac{R_1}{\Delta R} \int_0^x \frac{\partial \lambda_r}{\partial x} dx. \quad (2)$$

The static deformation of the free-standing arc x is determined by the intra-cavity optical power P_b , thus the wavelength tuning is controlled by P_b . The intra-cavity optical power is provided by the gain chip, and the power level is controlled by the gain currents. Supposed the gain current is I_1 , stable lasing at wavelength λ_1 is obtained when the force equilibrium is built up, corresponding to the free-standing arc's deformation x_1 . The force equilibrium in the laser cavity is re-built when gain current is changed to I_2 , and subsequently, the amount of the deformation is tuned to

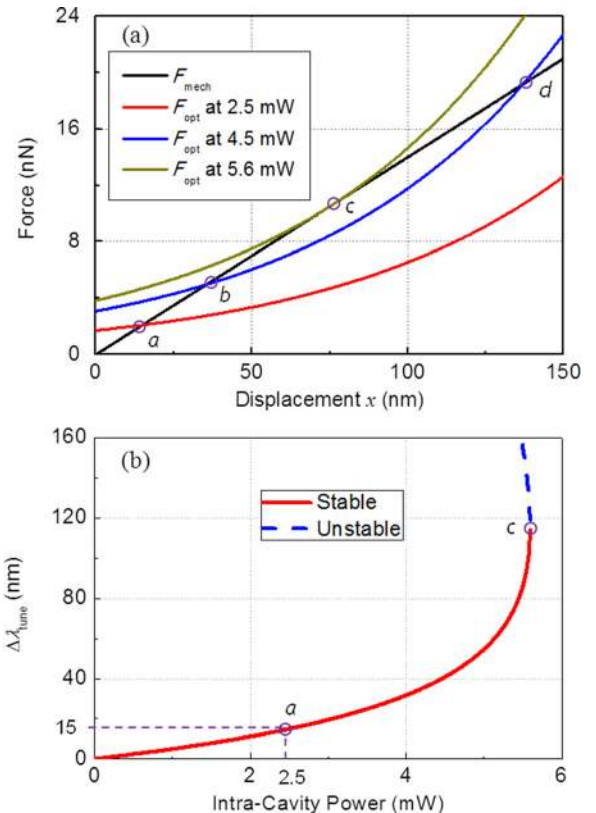


FIG. 2. (a) Deflection of the free-standing arc corresponding to different intra-cavity optical power P_L , achieved by the comparison of the optical force and the mechanical force; (b) the tuning amount of lasing wavelength $\Delta\lambda_{\text{tune}}$ as a function of the intra-cavity optical power.

x_2 and thus the lasing wavelength is tuned to λ_2 . The obtainable wavelength tuning range $\Delta\lambda_{\text{tune}}$ is a function of P_b as shown in Fig. 2(b). The stable and unstable wavelength tunings indicate the stable and unstable deformation x , respectively. Ideally, the maximum stable wavelength tuning range is 116 nm under an intra-cavity power of 5.6 mW. However, under large deformation condition, the van der Waals force becomes dominant when the free-standing arc is closely approaching to the dielectric layer. Moreover, the thermal-optic effect is unavoidable at relatively high-power condition. To weaken this disturbance, the opto-mechanical tunable laser is preferred to work at lower intra-cavity power (and thus small deformation): i.e., a 15-nm wavelength tuning range (~ 14.8 nm arc deformation) is obtained when the optical power increases from 0 to 2.5 mW.

The opto-mechanical coupled-ring reflector is fabricated on a silicon-on-insulator wafer. A commercial gain chip is bonded by using the flip-chip bonding technology. The SiO₂ inside the release window is partially removed by vapor hydrogen fluoride (HF). The SEM graph of the tunable laser is shown in Fig. 3(a). The nano-waveguide in the external cavity is highlighted with gray lines. The dimension of the gain chip is $250\ \mu\text{m} \times 250\ \mu\text{m} \times 100\ \mu\text{m}$. The zoom-in view of the free-standing arc is shown in Fig. 3(b). The released window on the driving ring has a dimension of $65\ \mu\text{m} \times 15\ \mu\text{m}$, and the cross-sectional length of the free-standing arc is $\sim 11\ \mu\text{m}$. The SiO₂ layer underneath the ring waveguide is $2.0\ \mu\text{m}$ before vapor HF etching. The air gap between the free-standing arc and the remaining SiO₂ layer can be controlled via the etching time (etching rate: 10 nm/min), thus a 160-nm air gap is formed after a 16-min etching.

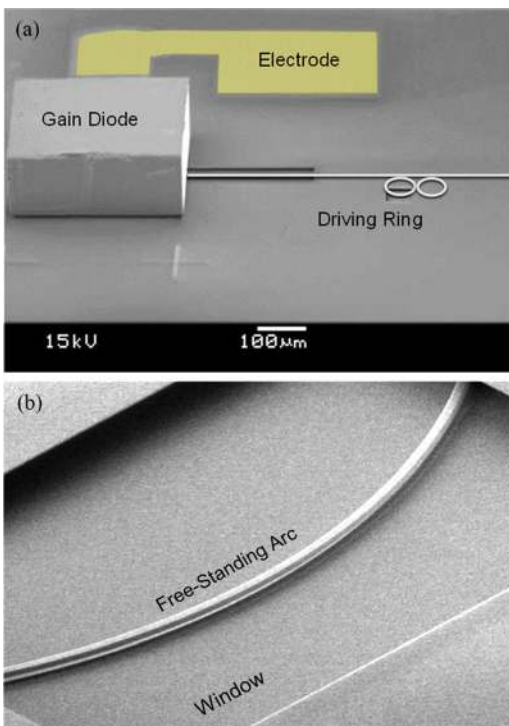


FIG. 3. SEM images of (a) the silicon chip tunable laser using an opto-mechanical coupled-ring reflector, and the gain chip is flip-chip bonded onto the silicon-on-insulator chip; (b) the zoom-in view of the free-standing arc in a released window.

In the experiments, the transmission and reflection spectra of the opto-mechanical coupled-ring reflector are measured by using a broadband light (power density: -43 dBm/0.02 nm), which is coupled in and out of the bus waveguide through the two tapered optical fibers, and the optical spectra are detected by an optical spectrum analyzer (OSA, Advantest Q8384) as shown in Fig. 4(a). The broadband light source covers the range from 1500 to 1610 nm. At $\lambda_3 = 1541.20$ nm, the left resonance-dip on the transmission spectrum results from ring 1, while the right resonance-dip results from ring 2. The resonance detuning of the ring resonators is 0.11 nm. A smaller resonance detuning of 0.06 nm is observed at $\lambda_2 = 1538.30$ nm. The resonance-dips of both rings almost merge at $\lambda_1 = 1535.48$ nm, corresponding to the peak reflectivity in the reflection spectrum. Therefore, it is the resonance of the coupled-ring reflector. The reflectivity at λ_1 is measured to be 78% (-2.1 dB). Once the free-standing waveguide deflects, the resonance of ring 1 is red-tuned while the resonance of ring 2 is remained constant. The resonance of the coupled-ring reflector changes from λ_1 to λ_2 and then to λ_3 with the increase of the intra-cavity optical power. Consequently, the lasing wavelength is tuned from λ_1 to λ_n , discretely.

To distinguish the opto-mechanical effect from the thermal-optic effect, a ring resonator with a $1.5\text{-}\mu\text{m}$ air gap of the free-standing arc is experimentally investigated by measuring the resonance shift of the driving ring. When the optical power injected into the bus waveguide is increased from 0 to 2.5 mW as shown in Fig. 4(b), the measured resonance shift is increased to 0.540 nm and 0.052 nm at 2.5 mW for $g_0 = 160$ nm and $1.5\ \mu\text{m}$, respectively. Since the opto-mechanical effect for the free-standing arc with an air gap of $1.5\ \mu\text{m}$ is extremely weak and negligible, the resonance shift

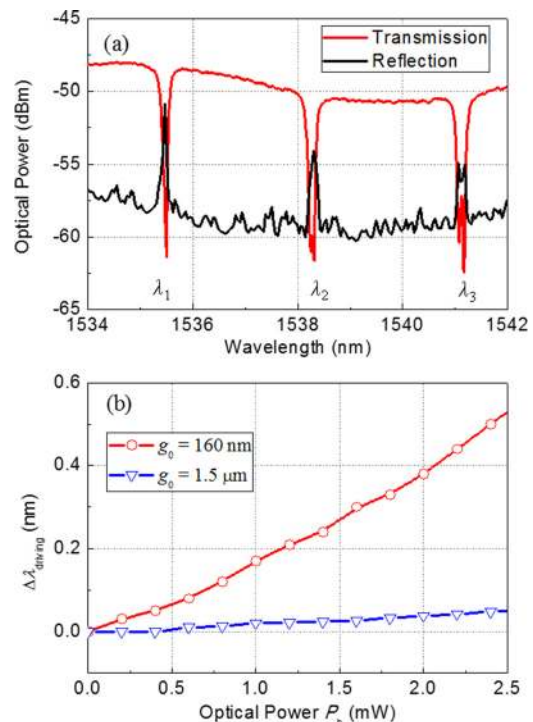


FIG. 4. (a) Measured transmission and reflection spectra of the coupled ring structure. The resonance of the fixed ring and the free-standing ring merges at λ_1 , and is differentiated slightly at λ_2 and λ_3 ; (b) the measured resonance shift of the driving ring when the optical power P_b is increased from 0 to 2.5 mW under two conditions: $g_0 = 160$ nm and $g_0 = 1.5\ \mu\text{m}$ (opto-mechanical effect is negligible).

of 0.052 nm is purely due to thermal-optic effect. Therefore, for the free-standing arc with an air gap of 160 nm, the contribution of the thermal-optic effect is just $\sim 9.6\%$, but the opto-mechanical effect dominantly contributes $\sim 90.4\%$.

To investigate the lasing performance, the packaged device is placed on a submount, connecting with a thermoelectric cooler, and its working temperature is kept at 25 °C. The gain diode has a 3-dB bandwidth of ~ 45 nm (1510–1555 nm) and a saturation output power of 7 dBm. The light emitted from the left facet of the gain diode is collected using a lens fiber and measured by the OSA. The threshold of the tunable laser is ~ 180 mA, and the gain diode is electrically pumped. The injection current of the gain diode is tuned above 180 mA in order to provide different intra-cavity powers. Figure 5(a) shows the single-mode lasing spectra under different gain currents. The lasing wavelength is discretely tuned, accompanying with the change in output powers. When the gain diode works at 210 mA, a single-mode lasing at $\lambda_1 = 1535.48$ nm is observed. Subsequently, $\lambda_2 = 1538.30$ nm, $\lambda_3 = 1541.15$ nm, $\lambda_4 = 1524.2$ nm, and $\lambda_5 = 1526.7$ nm lase at 238 mA, 260 mA, 295 mA, and 310 mA, respectively. Correspondingly, the output lasing power increases from -6.0 to -2.9 dBm, -1.4 dBm, and -0.8 dBm. The coupled-ring reflector has a 30-nm free spectral range due to the Vernier effect, thus there are two 30-nm tuning-periods within the 3-dB gain spectrum. As a result, the tuning of the lasing wavelength is non-monotonic due to the mode competition as shown in Fig. 5(b). The wavelength tuning is discrete with ~ 2.7 nm (340 GHz) channel space. The achievable SMSR (side mode suppression ratio) is kept around 30 dB during the opto-mechanical wavelength tuning. Under a constant gain-current, the lasing wavelength is stable with negligible wavelength shift due to the high mechanical damping of the free-standing arc. The tolerance for the gain-current fluctuation is ± 5 mA, and the gain

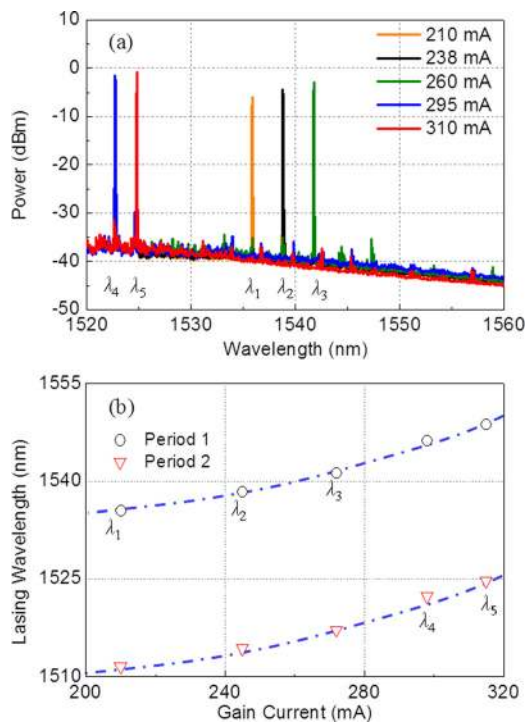


FIG. 5. Experimental results of (a) a series of single-mode lasing wavelength under different gain currents; (b) the process of the single-mode wavelength tuning of the opto-mechanical tunable laser.

current is slightly adjusted to obtain the finest phase match between the central reflective wavelength and one of the longitudinal modes. The lasing wavelengths and the output lasing power are stable with a standard deviation of ± 0.06 nm and ± 0.3 dB, respectively. The lasing wavelength changes nonlinearly with the intra-cavity optical power. The experimentally acquired lasing tuning range is 13.3 nm (1660 GHz). After calibration by deducting the contribution of the thermal-optic effect, the lasing wavelength tuning range caused by the opto-mechanical effect is 1500 GHz, which corresponds to an 11.8-nm deformation of the free-standing arc. Thus, the opto-mechanical lasing-wavelength tuning coefficient is 127 GHz/nm (nm is the unit of arc deflection).

In conclusion, an opto-mechanical coupled-ring reflector driven by optical force is used for an external-cavity tunable laser, whereby the lasing wavelength is controlled with an all-optical manner. A 13.3-nm wavelength tuning range with ~ 340 GHz channel space is demonstrated based on the opto-mechanical lasing-wavelength tuning coefficient of 127 GHz/nm. It shows a 30-dB SMSR, with its output power varies from -6.0 to -0.8 dBm. The demonstrated tunable laser provides potential applications not only in optical network but also in on-chip nanoparticle trapping, mass sensing, and biology detection.

¹M. C. Amann and J. Buus, *Tunable Laser Diodes* (Artech House, Boston, 1998).

²A. J. Ward, D. J. Robbins, G. Busico, E. Barton, L. Ponnampalam, J. P. Duck, N. D. Whitbread, P. J. Williams, D. C. J. Reid, A. C. Carter, and M. J. Wale, *IEEE J. Sel. Top. Quantum Electron.* **11**, 149–156 (2005).

³K.-H. Yoon, S. H. Oh, K. S. Kim, O.-K. Kwon, D. K. Oh, Y.-O. Noh, and H.-J. Lee, *Opt. Express* **18**, 5556–5561 (2010).

⁴B. Liu, A. Shakouri, and J. E. Bowers, “Wide tunable double ring resonator coupled lasers,” *Appl. Phys. Lett.* **79**, 3561–3563 (2001).

⁵S. Matsuo and T. Segawa, “Mirroring-resonator-based widely tunable lasers,” *IEEE J. Sel. Top. Quantum Electron.* **15**, 545–554 (2009).

⁶M. C. Y. Huang, Y. Zhou, and C. J. Chang-Hasnain, “A nanoelectromechanical tunable laser,” *Nat. Photonics* **2**, 180–184 (2008).

⁷X. M. Zhang, A. Q. Liu, D. Y. Tang, and C. Lu, “Discrete wavelength tunable laser using microelectromechanical systems technology,” *Appl. Phys. Lett.* **84**(3), 329–331 (2004).

⁸A. Q. Liu and X. M. Zhang, “A review of MEMS external-cavity tunable lasers,” *J. Micromech. Microeng.* **17**, R1–R13 (2007).

⁹H. Cai, A. Q. Liu, and X. M. Zhang, “A miniature tunable coupled-cavity laser constructed by micromachining technology,” *Appl. Phys. Lett.* **92**, 031105 (2008).

¹⁰M. L. Povinelli, M. Lončar, and J. D. Joannopoulos, “Evanescent-wave bonding between optical waveguide,” *Opt. Lett.* **30**, 3042–3044 (2005).

¹¹M. Li, W. H. P. Pernice, C. Xiong, T. Baehr-Jones, M. Hochberg, and H. X. Tang, “Harnessing optical force in integrated photonics circuits,” *Nature* **456**, 480–485 (2008).

¹²H. Cai, K. J. Xu, A. Q. Liu, Q. Fang, M. B. Yu, G. Q. Lo, and D. L. Kwong, “Nano-opto-mechanical actuator driven by gradient optical force,” *Appl. Phys. Lett.* **100**, 013108 (2012).

¹³J. Zhang, K. F. Macdonald, and N. I. Zheludev, “Optical gecko toe: Optically controlled attractive near-field forces between plasmonic metamaterials and dielectric or metal surfaces,” *Phys. Rev. B* **85**, 205123 (2012).

¹⁴Y. F. Yu, M. Ren, J. B. Zhang, T. Bourouina, C. S. Tan, J. M. Tsai, and A. Q. Liu, “Force-induced optical nonlinearity and Kerr-like coefficient in opto-mechanical ring resonators,” *Opt. Express* **20**, 18005–18015 (2012).

¹⁵B. Dong, H. Cai, G. I. Ng, P. Kropelnicki, J. M. Tsai, A. B. Randles, M. Tang, Y. D. Gu, Z. G. Suo, and A. Q. Liu, “A nanoelectromechanical systems actuator driven and controlled by Q-factor attenuation of ring resonator,” *Appl. Phys. Lett.* **103**, 181105 (2013).

¹⁶M. Ren, J. Huang, H. Cai, J. M. Tsai, J. Zhou, Z. Liu, Z. Suo, and A. Q. Liu, “Nano-opto-mechanical actuator and “pull-back” instability,” *ACS Nano* **7**, 1676–1681 (2013).

¹⁷I. Chremmos and N. Uzunoglu, “Reflective properties of double-ring resonator system coupled to a waveguide,” *IEEE Photonics Technol. Lett.* **17**, 2110–2112 (2005).